Chemical Engineering Journal 530 (2026) 173835

Contents lists available at ScienceDirect

Chemical Engineering Journal

journal homepage: www.elsevier.com/locate/cej

Nanoparticle-based delivery of DNAzymes to mitigate inflammatory responses in activated macrophages

Brandon Conklin, Sarah Nevins, Callan D. McLoughlin, Skylar T. Chuang, Joshua B. Stein, Yannan Hou, Munaifa Arif, Mehdi Kamali, Ki-Bum Lee *

Department of Chemistry and Chemical Biology, Rutgers, the State University of New Jersey, 123 Bevier Road, Piscataway, NJ, 08854, USA

ARTICLE INFO

Keywords:
Macrophage repolarization
Nucleic-acid delivery
Degradable nanoparticle
Calcium phosphate
Endosomal escape
Metabolic reprogramming

ABSTRACT

Macrophages are highly plastic cells that act as key regulators in the inflammatory process by releasing cytokines to facilitate immune cell infiltration, orchestrate various cellular responses, and help clear bacteria and cellular debris. In chronic inflammatory conditions, macrophages fail to polarize from a pro-inflammatory to an anti-inflammatory phenotype, and the constant inflammatory environment leads to an increase in both apoptosis and unprogrammed cellular death cascades that exacerbate the pathology To address this problem, we developed a biodegradable nanoparticle platform (PCaP NP) that encapsulates a nonimmunogenic nucleic acid in the form of a DNAzyme to suppress IRF5 expression, which promotes macrophage depolarization from a pro-inflammatory state. Our system is comprised of three unique components: 1) a calcium phosphate nanoparticle core designed for predictable biodegradability and optimal retention of nucleic acid payloads, 2) an IRF5-specific DNAzyme designed to silence the expression of IRF5 while mitigating adverse immunogenic responses, and 3) a poly (β-amino ester) (PBAE) polymeric coating to aid with endosomal escape, higher cellular interaction and uptake, and reduced NP-degradability at physiological pH. In this work, we have demonstrated the ability to transfect classically activated macrophages, directly suppress IRF5 expression and downstream cytokines, and cause metabolic changes that are indicative of an alternatively activated phenotype. These results suggest that PCaP NP offers a therapeutic approach to modulate inflammatory pathways in pro-inflammatory macrophages using a biodegradable and non-immunogenic platform.

1. Introduction

Inflammation is a complex and dynamic biological process characterized by multiple interacting pathways initiated in response to tissue injury, infection, or disease to promote healing and pathogen clearance. This process depends on intricate communication networks between immune cells and the surrounding tissue microenvironment. These cellular interactions involve the exchange of chemical signals and genetic mediators that orchestrate the inflammatory response, allowing immune cells to coordinate their activities and respond appropriately to various types of damage or pathogenic threats. Macrophages are an essential component of the innate immune system and are critical for producing inflammatory cytokines in response to disease and injury states. The proper balance of M1 and M2 phenotypes are critical [1]. These molecular cues are essential regulators of the inflammatory process, driving its initiation, maintenance, and ultimate resolution of inflammatory cascades. Furthermore, there is a clear connection between the production of pro-inflammatory cytokines, metabolic changes, and macrophage polarization. During the M1 state, macrophages have been well-reported to have increase glycolysis and a decrease in OXPHOS and fatty acid β-oxidation [2]. While in the M2 state, glycolysis decreases and there is an increase in OXPHOS and fatty acid β-oxidation. However, in a variety of diseases and injuries, macrophages will stay in the M1 state rather than transitioning to the M2 state. [3]. Therefore, therapeutic strategies aimed at modulating macrophage polarization toward an M2-like phenotype may hold promise for resolving chronic inflammation and promoting effective wound healing.

In recent years, nucleic acid-based therapies have become of major interest for the treatment of macrophages due to their specificity and scalability [4]. However, significant challenges must be addressed to realize their therapeutic potential such as stability and safety. Under

* Corresponding author at: Department of Chemistry and Chemical Biology, Rutgers, The State University of New Jersey, USA.
E-mail address: kblee@rutgers.edu (K.-B. Lee).

https://doi.org/10.1016/j.cej.2026.173835
Received 16 September 2025; Received in revised form 26 January 2026; Accepted 4 February 2026
Available online 5 February 2026

typical conditions, the delivery of unprotected nucleic acids proves ineffective or detrimental as nucleases, both inside and outside the cell, rapidly degrade these molecules in the presence of biological fluids. Moreover, the therapeutic efficacy of nucleic acids is often hampered upon cellular entry by their sequestration within endolysosomes, a process wherein the acidic pH and active enzymes within these organelles quickly degrade the nucleic acids. In particular, macrophages are notoriously difficult to transfect cells, as they have several membrane-bound, such as Toll-like receptors (TLRs), and cytosolic sensors designed to recognize nucleic acids as damage-associated molecular patterns (DAMPs) or pathogen-associated molecular patterns (PAMPs) [5]. TLR7 and TLR8 are specialized to recognize single-stranded RNA (ssRNA), TLR9 identifies unmethylated CpG motifs in DNA, and TLR3 detects double-stranded RNA (dsRNA) [6,7]. Similarly, cytosolic sensing pathways, including the cGAS-STING and RIG-I systems, detect foreign nucleic acids within the cytoplasm of macrophages. Specifically, cGAS-STING recognizes aberrant DNA, while RIG-I responds to viral RNA. By engaging these intracellular receptors, macrophages can mount an innate immune response to neutralize the detected threats [8,9]. The therapeutic efficacy of nucleic acids, such as miRNA, siRNA, and plasmid DNA, hinges on their efficient delivery to the appropriate intracellular compartment. Inefficient delivery can lead to endolysosomal entrapment, reducing therapeutic efficacy and potentially activating innate immune responses by engaging endosomal pattern recognition receptors. Therefore, carefully designing delivery strategies is crucial for therapeutic success and minimizing off-target effects.

To this end, one class of engineered nucleic acids designed to specifically recognize and cleave target messenger RNA (mRNA) is the ***DNA enzyme***, or ***DNAzyme***. Among these, the 10–23 DNAzyme is a well-studied variant known for its ability to bind and promote the site-specific cleavage of RNA transcripts [10]. Compared to RNA interference (RNAi) approaches, which depend on multiple endogenous cellular factors to operate effectively, DNAzymes only require a metal cofactor to achieve their catalytic functionality [11,12]. Furthermore, DNAzymes are composed of single-stranded DNA (ssDNA) and exhibit greater intrinsic stability than ssRNA because they lack the reactive 2′-hydroxyl group present in RNA. While this structural feature enhances their stability, it has also been observed that 10–23 DNAzymes do not facilitate TLR9 dimerization, thereby reducing their immunogenic potential. In contrast, RNAi-based therapies may inadvertently activate RIG-I, increasing the likelihood of an innate immune response [13–15]. Despite the inherent advantages of DNAzymes for applications in immune cell modulation, several challenges remain to be addressed before their full therapeutic potential may be realized. These challenges include optimizing their design for enhanced catalytic activity and target specificity, developing efficient delivery strategies to ensure intracellular access and localization, and achieving controlled activation within the complex biological environment of the target cell. While there have been recent advances in the modifications that can be implemented to increase the longevity and activity of the DNAzyme in vitro, many of these studies rely on transfection reagents and intracellular concentrations of divalent metal cofactors, ultimately resulting in poor kinetics and translatability [16,17].

To address the challenges in macrophage polarization as well as DNAzyme delivery, we developed a synergistic nanoparticle platform composed of biodegradable and biocompatible materials that can efficiently deliver DNAzymes directly into the macrophage cytoplasm. Our developed nanoparticle-based platform ensures proper intracellular release and catalytic activation by encapsulating and protecting the DNAzyme cargo during transport. As a result, this system enables the targeted downregulation of IRF5, a key transcription factor (TF) associated with inflammation, offering a robust strategy to modulate innate immune responses and improve therapeutic outcomes [18,19]. Specifically, IRF5 leads to an increase in pro-inflammatory cytokine production, such as TNFα, IL-6, and IL-1β, an increase in type 1 IFNs, and regulates glycolytic pathways through binding directly to genes involved in glycolysis [20,21]. By simultaneously effecting pro-inflammatory cytokine production and regulating metabolic pathways, IRF5 regulation can polarize macrophages. While IRF5 has been identified as a central regulator of the inflammatory response, inhibitors that interfere with IRF5 remain elusive, leading us to design a DNAzyme to specifically downregulate this clinically relevant target. Designing and synthesizing the nanoparticle platform involved a multi-step electrostatic assembly. First, calcium phosphate (CaP) nanoparticles were synthesized to encapsulate the IRF5-targeting DNAzyme. This encapsulation strategy protects the DNAzyme from degradation and facilitates its intracellular delivery. Next, the CaP nanoparticles were coated with an ionizable polymer PBAE. The proton sponge effect from the PBAE coating enhances cellular uptake and facilitates endosomal escape a crucial step to prevent sequestration and degradation of the DNAzyme within endo/lysosomal compartments. By enabling the release of functionally active DNAzymes directly into the cytosol, we ensure that the catalytic cleavage of target mRNA is both efficient and specific. Furthermore, as CaP degrades in acidic pH, Ca^{2+} is released from the particle in the endosome preventing the need of an alternate source of calcium. Taken together, this polymer-coated calcium phosphate nanoparticle (**PCaP NP**) can overcome several limitations associated with DNAzymes and macrophage delivery by: (i) providing a sufficient source of divalent calcium ions necessary to activate the DNAzyme, (ii) encouraging cellular uptake and endosomal escape of the PCaP NP, and (iii) targeting *ifr5* directly with notable downstream effects [Fig. 1 A-C]. Moreover, PCaP NPs are highly biodegradable and biocompatible, leading to minimal toxicity and immunological concerns as opposed to other commonly used methods where the degradation byproducts can trigger unwanted immune responses [22]. To address the design constraints of the IRF5 DNAzyme, an open-source software (MXfold2) was utilized to predict the secondary structure of the target mRNA, and the DNAzyme was designed to target non-paired regions of the IRF5 mRNA [23]. By applying this nanoconstruct, we demonstrated the capacity to target and cleave *irf5* within classically activated macrophages. This intervention increased oxidative phosphorylation (OXPHOS), improved mitochondrial function, reduced pro-inflammatory cytokines levels, as well as prevented activation of the cGAS-STING and RIG-I pathways. In addition, we observed broader metabolic and transcriptomic shifts consistent with an alternatively activated macrophage phenotype, underscoring the platform's potential to modulate immune cell behavior at the molecular level [Fig. 1D, E].

2. Results and discussion

2.1. Synthesis, design, and characterization of irf5-specific DNAzymes and polymer-coated calcium phosphate nanoparticles (PCaP NPs)

To maximize the therapeutic potential of our DNAzyme-loaded PCaP NP platform, we aimed to investigate and optimize an efficient design of an *irf5*-specific DNAzyme as the primary therapeutic payload of the platform. We began by dividing the *irf5* sequence into 750 base pair (bp) fragments and inputted these fragments into the open-source software MXfold2 to predict the secondary structure of the mRNA sequence (Fig. 2 A) [23]. From these secondary structures, we identified potential target sites in the mRNA that had guanine (G) and uracil (U) residues adjacent to one another in a location that was not self-paired (i.e., located in either a loop or bulge) to mitigate competitive inhibition with the DNAzyme. Moreover, BLAST results for these DNAzymes and their target site did not show a high similarity to any other known DNA sequence, illustrating that the designed DNAzymes were highly specific to the IRF5 target sequence. By optimizing the DNAzyme design in this manner, its enzymatic activity was maximized while maintaining strict specificity for the intended target. This approach also reduced the likelihood of secondary structure formation and product inhibition, ensuring the DNAzyme functioned efficiently and effectively once delivered [24,25].

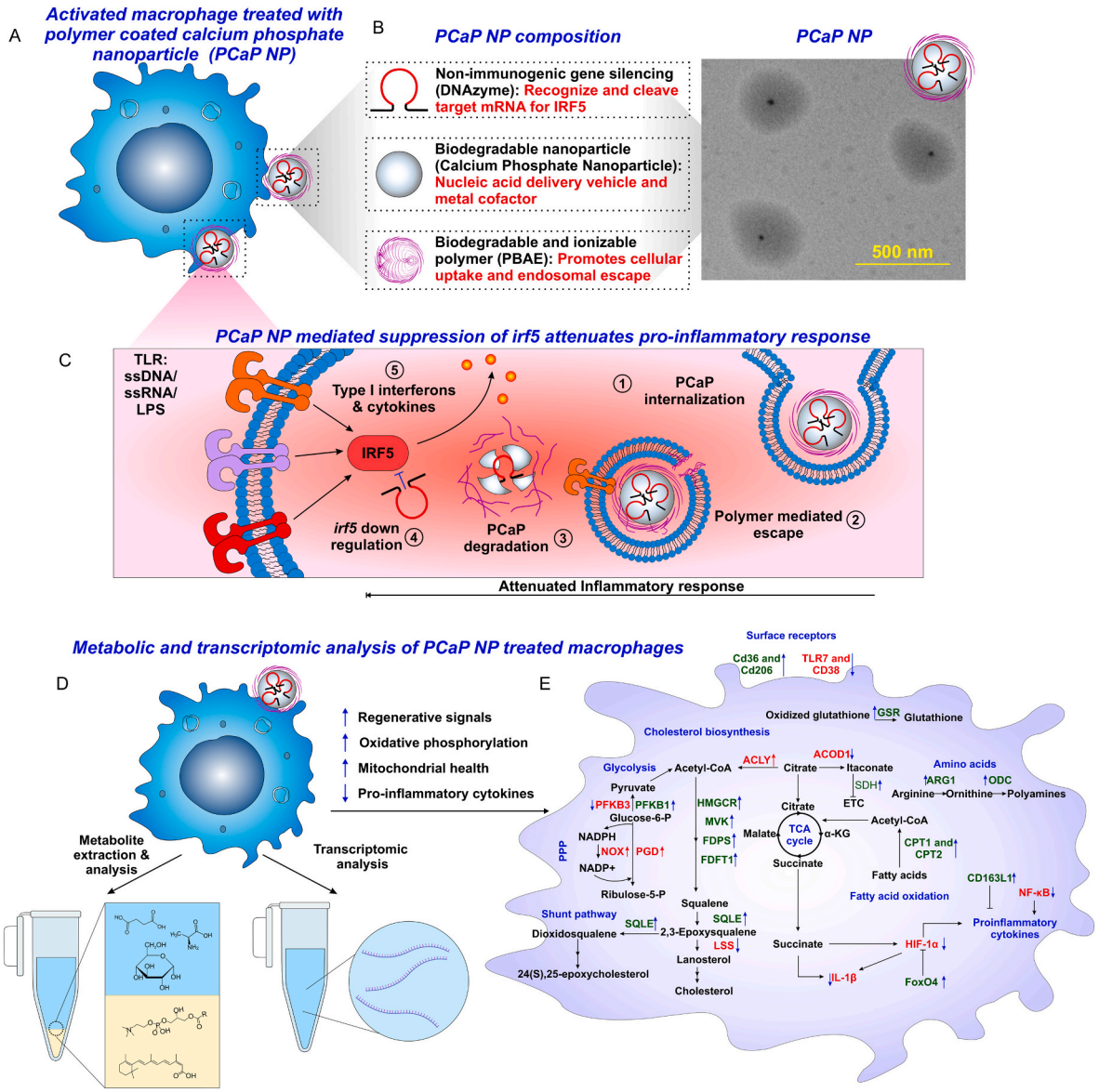

Fig. 1. Nanoparticle-mediated attenuation of inflammatory responses in classically activated (M1) macrophages. A) Schematic illustration of THP-1 monocyte-derived M1-like macrophages being treated with PCaP NP. B) Illustration and TEM highlighting the key components that compose the PCaP NP platform and demonstrating how they synergistically contribute to the attenuation of inflammation. C) The PCaP NP platform is internalized by M1-like macrophages, where it can undergo polymer-mediated endosomal escape and enter the cytoplasm. The platform then degrades and releases Ca^{2+} to activate the DNAzyme to cleave mRNA for *irf5*, thereby preventing the expression of type I interferons and cytokines without activating membrane-bound sensors (i.e., TLRs). D) Metabolic and transcriptomic analysis of PCaP NP-treated M1-like macrophages reveals changes in the bioenergetics and cytokine activity that are indicative of the suppression of inflammation. E) Metabolic changes were observed in classically activated macrophages treated with PCaP NP.

To determine the optimal design, the most effective DNAzyme construct we identified was modified such that an extra two nucleotides were added to each flanking binding arm, and a deactivated control was created by replaying the thymine in position 4 of the catalytic loop with a cytosine (Table S1) [26]. These constructs were referred to as (7 + 7), (9 + 9), and T4C owing to the length of their binding arms and the nucleotide replacement, respectively. It was revealed by a denaturing PAGE gel that the (9 + 9) construct initially had significantly faster enzymatic kinetics but was only able to complete approximately 8 turnovers, whereas the (7 + 7) construct successfully cleaved 96.3% of the RNA substrate. Similarly, we noted a 12.4% decrease in the RNA substrate when incubated with the T4C construct, which is attributed to the DNAzyme binding to but not releasing the substrate (Fig. 2B and Fig. S1). For our purposes, the (7 + 7) construct was more efficient than the (9 + 9) construct in respect to the overall *irf5* mRNA cleavage, even though the latter construct displayed faster binding and cleavage kinetics. Concentration-dependent studies were also conducted to determine the optimal concentration of $CaCl_2$ when synthesizing the CaP particle (Fig. 2C). The concentration-dependent kinetics of *irf5* mRNA binding and cleavage by the (7 + 7) construct was explored over a concentration of $CaCl_2$ ranging from 100 to 500 mM. As expected, higher concentrations of Ca^{2+} ions in the presence of our selected DNAzyme led to overall faster and more complete *irf5* mRNA cleavage. The thoughtful DNAzyme design and tailored PCaP NP optimization laid the framework for our PCaP NP-DNAzyme delivery system, increasing the potential for our therapeutic platform to selectively and efficiently downregulate *irf5* in macrophages in vitro.

The synthesis of DNAzyme-encapsulated CaP NPs was modified from previously reported studies where two separate emulsions were formed using cyclohexane, Igepal CO-520, and water (Fig. 2D) [27]. The

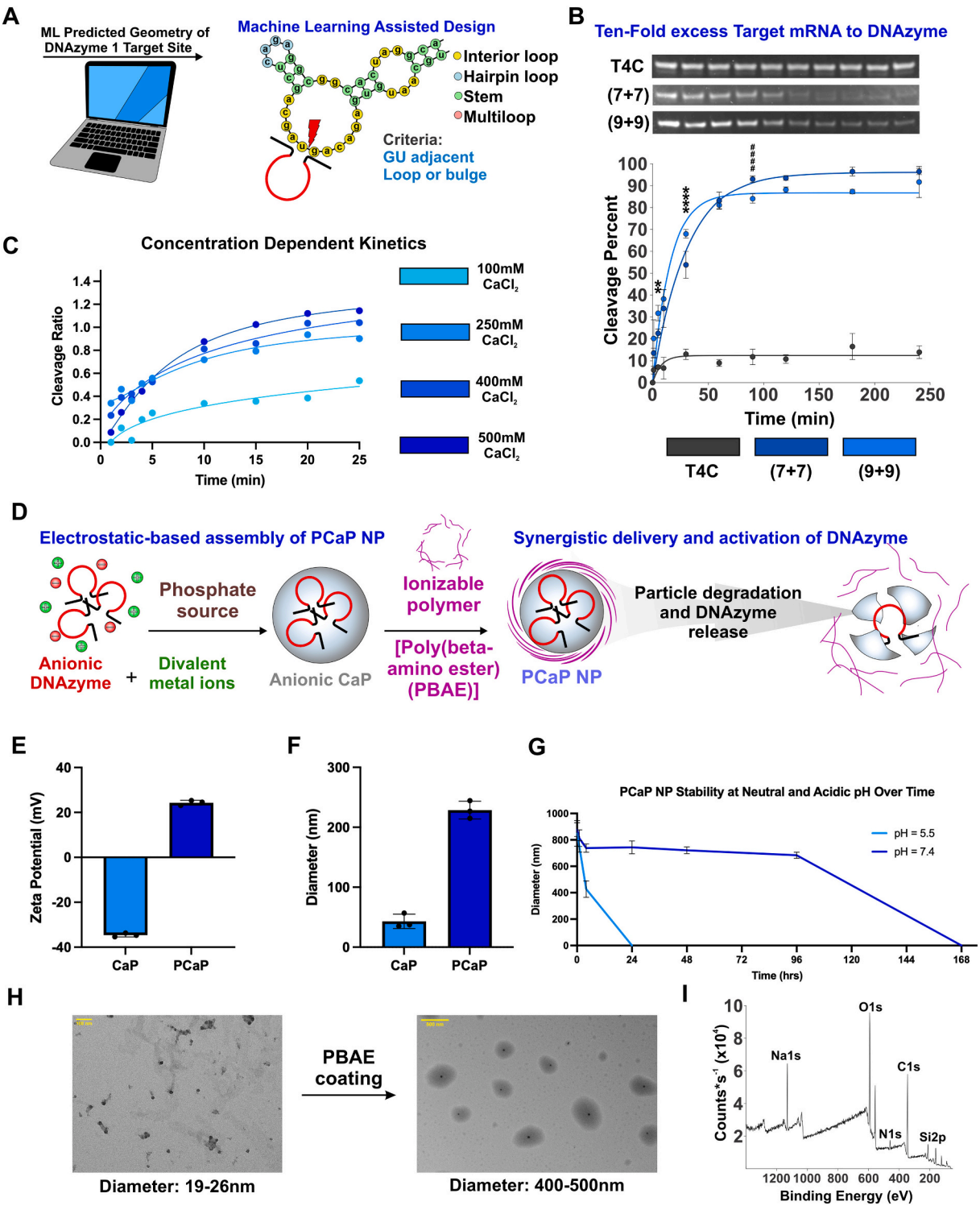

Fig. 2. Overall design, characterization, and optimization of *irf5*-DNAzymes and PCaP NP platform. A) Predicted geometry of target mRNA sequence using MXfold2. 10-23 DNAzymes cleave between guanine and cytosine, and MXfold2 aided in GU cleavage sites that were not self-paired to reduce competitive inhibition. B) Representative denaturing PAGE gel and associated cleavage kinetics of DNAzyme variants in the presence of excess RNA substrate for deactivated DNAzymes (T4C) and DNAzymes of varying binding arm length [(7+7) and (9+9)] (n = 3). C) Denaturing PAGE gel investigating the calcium concentration-dependent cleavage kinetics of *irf5* mRNA substrate. D) Schematic illustration of the electrostatic-based assembly of PCaP NP. E) Zeta potential measured prior to and after polymeric coating CaP (n = 3). F) DLS measurements prior to and after polymeric coating of CaP (n = 3). G) DLS measurements of PCaP NPs in neutral (pH = 7.4) and acidic (pH = 5.5) conditions over 7 days. H) TEM images of bare CaP and PCaP NP, individual CaP particles can be observed being fully coated with PBAE. Scale bars are 100 nm and 500 nm, respectively. I) XPS demonstrating the presence of nitrogen species on the surface of PCaP NP, further confirming the successful coating of PCaP NP. Mean ± SEM, one-way ANOVA, turkey test, and t-test. *$P < 0.05$; **$P < 0.01$; ****P

encapsulation efficiency of the DNAzyme into CaP was found to be approximately 26 ± 1.79% via an agarose DNA gel (Fig. S2). Following the formation of CaP, we introduced a cationic polymer (PBAE) that was electrostatically attached to the surface of the NP to promote cellular internalization and endosomal escape (Fig. S3). Several methods were used to validate the encapsulation of CaP within PBAE to create the PCaP NP platform. First, zeta potential measurements were collected, and we noted a significant increase ($P < 0.0001$) in the charge of the particle following PBAE coating and activation (Fig. 2E). Next, dynamic light scattering (DLS) revealed a significant increase in particle size following PBAE coating ($P < 0.0001$) (Fig. 2F). Lastly, we investigated the overall stability of the PCaP NP platform in physiological conditions, both at neutral and acidic pH at 37 °C (Fig. 2G and S4). Over 7 days, the stability of the PCaP NP was maintained in neutral pH conditions with minimal degradation until after 4 days, while in acidic conditions, the NP was degraded within 24 h. This property and selective degradation was expected, as the CaP core of the NP was predicted to degrade in acidic conditions, similar to the early endosome microenvironment. In the physiological buffers utilized, we acknowledge the increase in size from the localized aggregation, which is quite common for CaP-based NPs [28]. Transmission electron microscopy (TEM) allowed for the visualization of individually coated CaP NPs within a polymeric matrix (Fig. 2H). Moreover, the surface of PCaP NP was analyzed via X-ray photoelectron spectroscopy (XPS) to identify nitrogen species indicative of PBAE coating (Fig. 2I). When taken together, these findings are characteristic of a successful CaP synthesis and subsequent PBAE coating. Additionally, we wanted to highlight the modularity of the PCaP NP platform by doping various divalent metal ions into the CaP NP to improve biological and material properties. Specifically, we chose to dope Zn^{2+} and Mn^{2+}, as the former is known to have anti-bacterial and anti-viral properties [29,30], while the latter has been shown to increase the catalytic activity of the encapsulated DNAzyme and has been shown to accelerate wound healing [12,31]. The ability to dope these divalent ion species into CaP NPs was shown via ICP-MS (Fig. S5). Besides these immediate findings, our results highlight potential avenues for enhancing the system's performance through the modularity provided by divalent metal doping, which could further fine-tune the nanoparticle's properties and therapeutic efficacy.

2.2. Optimizing the IRF5 DNAzyme to attenuate inflammatory responses in classically activated macrophages

To design an efficient system for macrophage polarization, a variety of parameters were optimized in vitro including the DNAzyme sequence, DNAzyme length, delivery concentration and delivery time. To this end, commercially available Lipofectamine™ 3000 was used to deliver the three DNAzyme constructs into classically activated macrophages (Fig. 3A). RT-qPCR revealed the first construct had the most significant decrease in *irf5* expression ($P < 0.0001$) and downstream reduction in TNF-α ($P < 0.01$) relative to the control and other two constructs (Fig. 3B

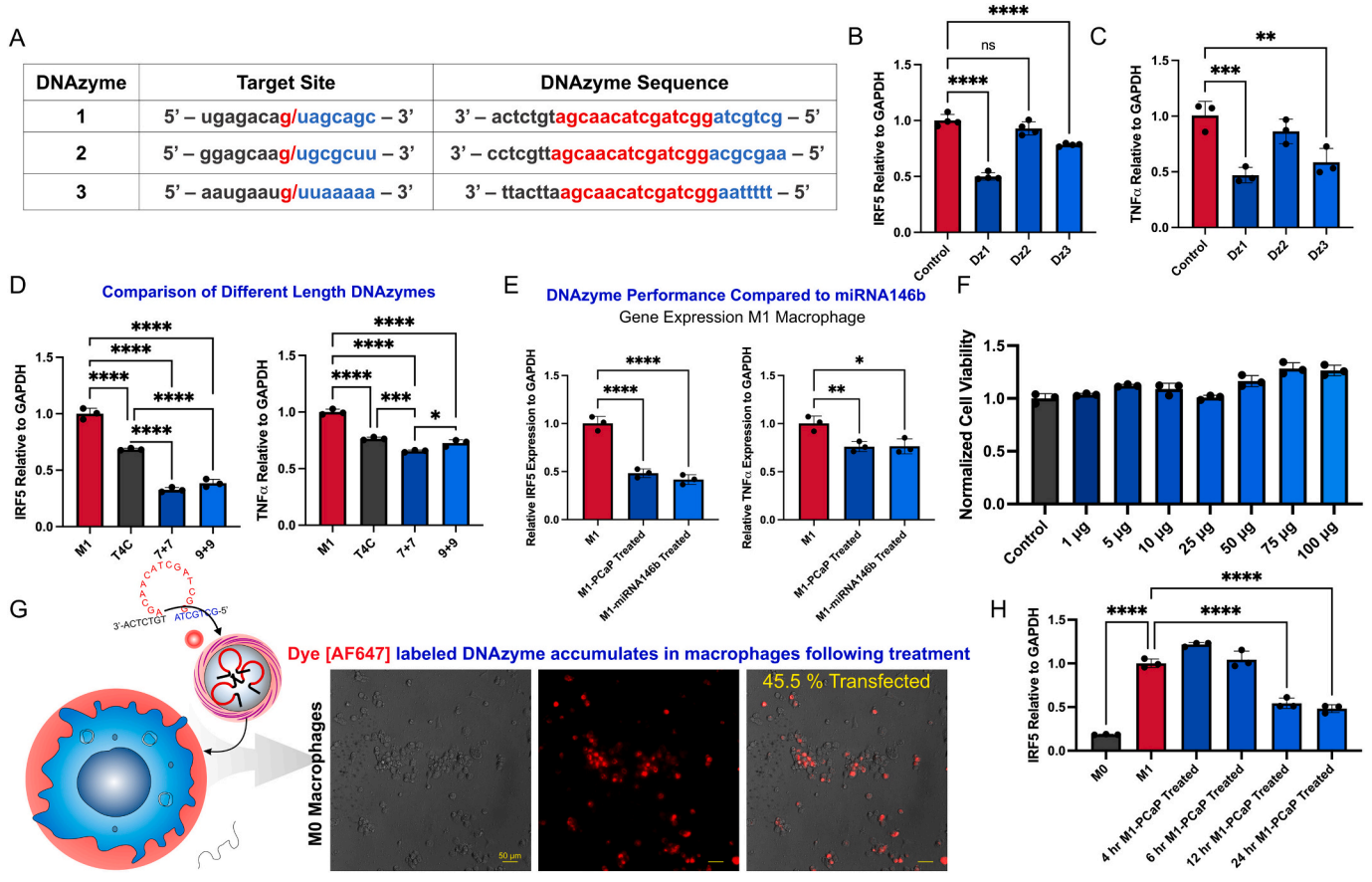

Fig. 3. Optimization of IRF5 DNAzyme attenuated inflammatory response in activated macrophages. A) DNAzyme construct designs and target sequence: the black, red, and blue correspond to the left binding arm, conserved catalytic loop, and right binding arm, respectively. RT-qPCR of B) *irf5* ($n = 4$) and C) *tnf-α* ($n = 3$) following Lipofectamine™ 3000 delivery of activated DNAzyme constructs to classically activated macrophages (LPS and IFN-γ) highlighting the most effective construct. D) Comparison of an inactive DNAzyme, as well as two different lengths of the active DNAzyme in regard to down-regulating *irf5* and *tnf-α* ($n = 3$). E) Comparison of the active DNAzyme to miRNA146b in regard to down-regulating *irf5* and *tnf-α* (n = 3). F) Cell viability was measured using Presto Blue following treatment of M1-like macrophages with various concentrations of PCaP NP (n = 3). G) Schematic illustration and images demonstrating the internalization of dye-labeled PCaP NP in inactivated macrophages. Scale bar 50 μm. H) Time dependent effect of PCaP NP treatment on *irf5* mRNA levels (n = 3). Mean ± SD, one-way ANOVA, and turkey test. *$P < 0.05$; ***$P < 0.001$; ****$P < 0.0001$; n.s. not significant.

and C). As such, all subsequent experiments used the first DNAzyme construct encapsulated within the PCaP NP, and analysis was conducted 24 h post-treatment. To further confirm the effects of length and RNA cleavage ability, (7 + 7), (9 + 9), and (T4C) IRF5 and TNFα mRNA levels were determined with RT-qPCR. There was a significant decrease ($P < 0.001$) in *irf5* and *tnf-α* expression for both the (7 + 7) and (9 + 9) constructs relative to the control (Fig. 3D). While not significant ($P > 0.05$), the (7 + 7) construct outperformed the (9 + 9) construct in suppressing *irf5*. These results determined that the (7 + 7) DNAzyme construct was the most kinetically and biologically efficient for downregulating *irf5*.The PCaP NP platform was compared to miRNA146b delivered with Lipofectamine™ 3000, which has previously been shown to target *irf5* [32]. Both *irf5* and *tnf-α* were significantly downregulated in classically activated macrophages ($P < 0.0001$), but there was not a significant change between the PCaP NP and miRNA146b treated conditions ($P < 0.05$) (Fig. 3E). The PCaP NP platform did not demonstrate toxicity and significantly ($P < 0.0001$) improved the viability of pro-inflammatory THP-1 macrophages that were activated with lipopolysaccharide (LPS) and interferon-gamma (IFN-γ) (Fig. 3F). We attribute this increase in viability to PCaP NP polarizing the classically activated macrophages to an anti-inflammatory phenotype.

Interestingly, macrophages are notoriously challenging to transfect, as they possess both cytosolic and membrane-bound sensors that can rapidly detect foreign genetic material. Activation of these sensors often triggers innate immune responses, making it challenging to deliver and express exogenous nucleic acids within these cells [6,8]. Despite this, we clearly demonstrated using a fluorescently labeled DNAzyme that PCaP NP successfully transfected 45.5% of macrophages, which was determined using CellTagging, an image-based method previously reported by the Morris group to quantify signal localization in cells (Fig. 3G) [33,34]. Finally, to look at time-dependent effects of PCaP NP on *irf5* with RT-q-PCR, it was delivered for 4, 6, 12, and 24 h (Fig. 3H). Significant downregulation of *irf5* ($P < 0.0001$) was seen after both 12 and 24 h.

cGAS/STING and RIG-I can recognize foreign nucleic acids and lead to the activation of IRF3, NF-κB and IRF7, while IRF5 downregulation reduces the expression of pro-inflammatory cytokines (Fig. 4A). Therefore, the effects on PCaP NP were studied on pro-inflammatory cytokines, a Type 1 IFN, and cGAS/STING activation. After finalizing optimization of the DNAzyme and PCaP NP delivery concentration and time, IRF5 downregulation was studied in a model inducing an M1 phenotype in the THP-1 monocytes differentiated to macrophages. *Irf5* mRNA was significantly downregulated following PCaP MP delivery to M1 macrophages ($P < 0.0001$) (Fig. 4B). To test the effects of PCaP NP on M0 and M2 *irf5* mRNA, inactivated macrophages and alternatively activated macrophages were treated with PCaP NP which showed significant downregulation in M2 macrophages and no significant difference in M0 macrophages (Fig. S7A and B). Western blot results for IRF5 protein levels gave no significant change in both the M0 and M2 conditions.

As previously noted, macrophages are hard-to-transfect cells that have developed various methods to sense foreign nucleic acids. To this end, we sought to verify that the PCaP NP platform could be successfully internalized by activated macrophages and effectively escape from endosomal compartments. To accomplish this goal, a dye (Alexa Fluor 647) labeled DNAzyme (Table S1) was delivered via the PCaP NP platform and tracked in relation to endosomes labeled with Rab5 (Fig. S6A). Over four hours, we analyzed immunofluorescent images to assess the distribution of DNAzymes relative to endosomal compartments. By generating a color scatter plot and calculating the Pearson correlation coefficient, we observed reduced colocalization between the DNAzymes and endosomes, proving that the DNAzymes successfully escaped the endosomal environment (Fig. S6B and S6C).

The ability to promote endosomal escape from the PCaP NP platform was further demonstrated by noting a decrease in activated macrophage markers downstream of IRF5, including *irf7* and *ifn-β*, highlighting the ability of this platform to modulate innate immune responses (Fig. 4C and D). Furthermore, IRF7 is activated downstream of Rig-I, which is indicative of recognition of dsRNA, another advantage over siRNA-based systems. IFN-β upregulation is further indicative of nucleic acid detection by either cGAS-STING or Rig-I, as it is downstream of both. Therefore, the significant downregulation of *irf7* and *ifn-β* mRNA levels are indicative that neither cGAS-STING or Rig-I are activated. Due to the significant downstream effects of IRF5 downregulation on IFN-β, the effects of PCaP NP treatment on *ifn-β* in M0 and M2 macrophages was also tested with RT-q-PCR. Significant downregulation of *ifn-β* was seen in M0 treated macrophages ($P < 0.01$) while it was upregulated in M2 treated macrophages ($P < 0.001$) (Fig. S6C and D). Additionally, there was a significant ($P < 0.01$) decrease in *nlrp3* expression in PCaP NP-treated classically activated macrophages compared to the untreated condition (Fig. 4E). Previous studies have shown that the *nlrp3* inflammasome is upregulated following the escape of cargo from late endosomal or lysosomal compartments. Conversely, lower levels of this marker are associated with early endosomal escape, suggesting that prompt release of delivered materials may help avoid activating this inflammatory pathway [35]. Western blot demonstrated a significant downregulation of IRF5 ($P < 0.001$) and the pro-inflammatory cytokine IL-1β ($P < 0.05$) in the PCaP NP treated classically activated macrophages compared to the M1 control group (Fig. 4F, G, and H). IRF5 was not detected in the inactivated macrophages. Western blot was used to confirm the effects of PCaP NP on IRF5 protein levels when treated to inactivated and alternatively activated macrophages as well and showed no significant difference for either condition (Fig. S6E, F, G, H, and S8). *Ccl2* mRNA levels were also significantly downregulated as quantified by RT-q-PCR ($P < 0.0001$) (Fig. 4I). IRF3 and NF-κB are activated through cGAS/sting activation. Therefore,RT-q-PCR was utilized to study cGAS/STING activation and anti-inflammatory effects where significant *irf3* ($P < 0.05$) and *nf-κb* ($P < 0.0001$) mRNA downregulation was confirmed(Fig. 4J and M). NF-κB, another key TF in the inflammatory cascade, protein levels were quantified with western blot and showed a significant decrease in the NF-κB protein levels ($P < 0.001$) (Fig. 4K and L). Increased production of inflammatory cytokines, such as TNF-α, leads to an increase in NF-κB signaling creating a positive feedback loop between the two [36]. Furthermore, a decrease in NF-κB signaling has been shown to support NLRP3 inflammasome downregulation as NF-κB signaling induces the production of NLRP3 while a reduction in NF-κB restricts NLRP3 inflammasome activation [37]. As well as NF-κB decreasing as a downstream effect of IRF5 downregulation, NF-κB levels are regulated by cGAS-STING and Rig-I. Along with NF-κB, the cGAS-STING pathway regulates IRF3 as well. The significant downregulation of IRF3 with PCR further specifies this pathway was not activated. Finally, western blot was run on cGAS, STING, and pSTING (Fig. 4N). cGAS protein levels were quantified relative to beta actin and showed a significant decrease ($P < 0.01$) upon PCaP NP treatment to the M1 cell model (Fig. 4O). pSTING and sting were quantified relative to beta actin and the ratio of pSTING/STING was determined in each of the conditions (Fig. 4P). Although pSTING/STING ratio downregulation was not significant, it is important to note that the pathway was not activated by PCaP NP treatment. Furthermore, cGAS can modulate M1 macrophage polarization, so the downregulation of cGAS is due to the phenotypic shift in the macrophages from an M1 state. Despite their similar performance, we hypothesize that the PCaP NP platform would be less immunogenic than miRNAs, which have been shown to bind and activate TLR3, TLR7, and TLR8, since DNAzymes do not serve as ligands for these toll-like receptors [7]. Furthermore, TLR3, TLR7, and TLR8 activation by ssRNA leads to IRF7 and NF-κB upregulation which PCaP NP delivery was able to downregulate as previously discussed.

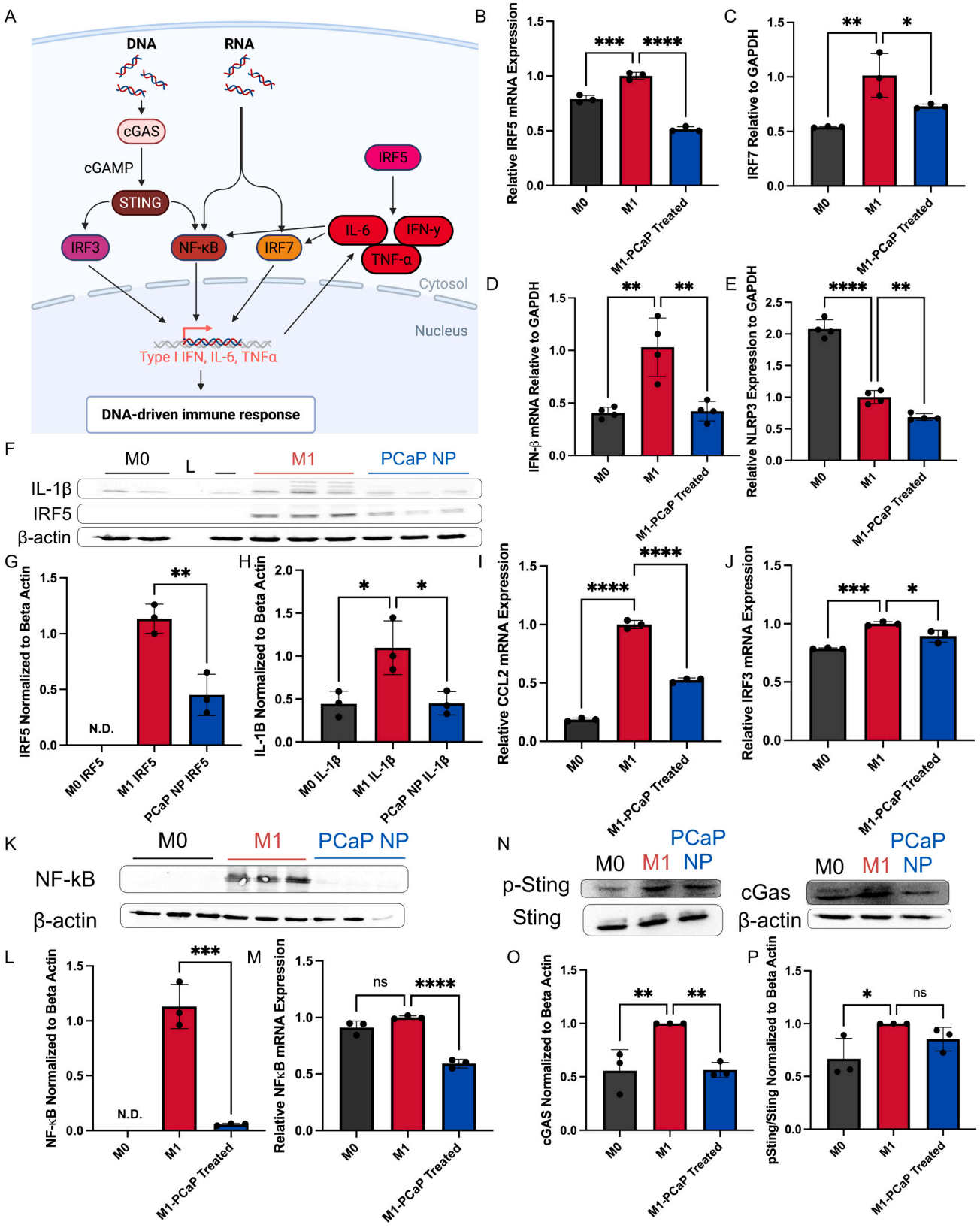

Fig. 4. Optimized IRF5 DNAzyme attenuated inflammatory response in activated macrophages. A) Schematic showing IRF5-mediated inflammation. RT-q-PCR of B) *irf5*, C) *irf7*, D) *ifn-β*, and E) *nlrp3* relative to *gapdh*. F) Western blot of IRF5, IL-1β, and Beta Actin. Quantification of G) IRF5 and H) IL-1β protein levels relative to Beta Actin. RT-q-PCR of I) *ccl2* and J) *irf3* relative to *gapdh*. K) Western blot of NF-κB and Beta Actin. L) Quantification of NF-κB protein levels relative to Beta Actin. M) RT-q-PCR of *nf-κb*. N) Western blot of P-STING, STING, cGAS, and Beta Actin. Quantification of O) cGAS and P) pSTING/STING protein levels relative to Beta Actin. Mean ± SD, one-way ANOVA, and turkey test. $^{*}P < 0.05$; $^{***}P < 0.001$; $^{****}P < 0.0001$; n.s. not significant.

2.3. Assessing macrophage health and bioenergetics via analysis of metabolomic and lipidomic markers

In this section, we describe how metabolomic and lipidomic markers were tested to evaluate macrophage health and bioenergetics. By examining shifts in metabolic profiles and lipid composition, we aimed to gain insight into the cellular state, energy utilization, and functional capabilities of macrophages following treatment interventions. Immunometabolism studies have revealed the methods macrophages use to generate energy vary depending on their activation state. Specifically, activation of macrophages in response to bacterial infections or viruses is metabolically demanding and relies on glucose metabolism for fast ATP production. Due to the disruption of the tricarboxylic acid (TCA) cycle in macrophages, there are notable alterations in metabolites including an accumulation of citrate and succinate that result in lipid biosynthesis, as well as dysregulated ATP:AMP cytosolic ratios which indicate impaired mitochondrial function. Additionally, other biomarkers indicative of an M1-like phenotypic state include the activation of the transcription factors such as HIF-1α, a loss of mitochondrial membrane potential (ΔΨm), and the upregulation of pro-inflammatory genes [38,39]. Conversely, alternatively activated macrophages utilize OXPHOS and fatty acid oxidation (FAO) in addition to an undamaged TCA cycle [40]. It has also been noted that alternatively activated macrophages have higher glycolytic capabilities than their inactivated counterpart but less so than classically activated macrophages; however, this bioenergetic pathway is not necessary to drive the anti-inflammatory state [41,42]. We hypothesized that delivering PCaP NPs to classically activated macrophages would induce a discernible shift in their bioenergetic profile. Given that IRF5 typically enhances glycolysis and stimulates the release of pro-inflammatory cytokines, downregulating this transcription factor should prompt metabolic reprogramming toward alternative energy pathways and diminish a pro-inflammatory phenotype [21]. This was accomplished by a multifaceted approach whereby quantitative nuclear magnetic resonance spectroscopy (qNMR) was used to quantify several water-soluble metabolites and mass spectrometry was implemented to quantify hydrophobic lipid-based metabolites.

Classically activated macrophages treated with PCaP NPs were lysed, and aqueous metabolites were collected to be analyzed by qNMR (Fig. 5A and Fig. S9). From the aqueous fraction, we quantified 19 metabolites and used these metabolites to demonstrate the PCaP NP-treated macrophages manifested themselves as a distinct population that was unique from inactivated and classically activated macrophages (Fig. 5D). Loading scores were determined from partial least squares discriminate analysis (PLS-DA) to identify key metabolites that aided in classifying the various macrophage populations. From the loading scores, we identified the top 6 aqueous metabolites to be (i) glycine, (ii) taurine, (iii) glucose, (iv) succinic acid, (v) glutathione, and (vi) creatine (Fig. 5D and Fig. S10). Interestingly, in macrophages, glycine has been shown to promote an alternatively activated phenotype by preventing the activation of NF-κB [43]. Similarly, taurine has been shown to prevent metabolic shifts to glycolysis while encouraging mitophagy, succinic acid promotes angiogenesis, and creatine inhibits JAK2/STAT1 pathways while upregulating STAT6 expression, all of which contribute to the anti-inflammatory phenotype [44–46]. In our PCaP NP-treated conditions, these metabolites were all detected and quantified to increased levels when compared to the inactivated and classically activated conditions (Fig. S10). Conversely, the antioxidant glutathione has been associated with classically activated macrophages [47]. Finally, the ATP:AMP ratio and amount of glucose per condition were quantified. It was found that the ATP:AMP ratio was significantly decreased in the classically activated conditions ($P < 0.01$) relative to the inactivated condition. However, following PCaP NP treatment, the ATP:AMP ratio was restored to levels comparable to the inactivated macrophages (Fig. 5B). This outcome is indicative of the reestablishment of healthy mitochondrial activity as well as a reduction in the rate of glycolysis, most often associated with classically activate macrophages. Moreover, the amount of glucose was found to be elevated significantly in the PCaP NP-treated condition relative to both the inactivated and classically activated conditions ($P < 0.01$) (Fig. 5C).

Since increased glucose uptake is associated with classically activated macrophages, we decided to study the mitochondrial membrane potential to gain further insight into the health and activity of the mitochondria in treated macrophages. Changes in mitochondrial membrane potential are linked with apoptosis, and depolarization of the membrane results in the release of apoptotic factors and a loss of OXPHOS [48]. Quantification of fluorescent images revealed that there was a significant decrease ($P < 0.001$) in the membrane polarization of classically activated compared to inactivated macrophages. Furthermore, the membrane potential significantly increased in classically activated macrophages after PCaP NP treatment, acting as the electrochemical gradient driving OXPHOS ($P < 0.01$) (Fig. 5J and K). Finally, the transcription factor HIF-1α was downregulated significantly ($P < 0.01$) in PCaP NP-treated classically activated macrophages compared to untreated classically activated macrophages, restoring similar levels as observed in the inactivated macrophage condition (Fig. 5L). In macrophages, HIF-1α plays an important role by downregulating OXPHOS and promotes glycolysis to conserve oxygen and maintain ATP production, typically observed in classically activated macrophages. Taken together, these shifts in the metabolic profile of treated classically activated macrophages are indicative of the macrophages adopting an alternatively activated phenotype relying on OXPHOS rather than glycolysis, demonstrating the feasibility of PCaP NP to diminish the classically activated phenotype.

Lipidomic studies leveraging mass spectrometry were further utilized to highlight the changes in the metabolic profile of inactivated macrophages, untreated classically activated macrophages, and treated classically activated macrophages. Lipophilic metabolites were isolated from the organic phase following cell lysis and extraction prior to performing mass spec (Fig. 5F). The collected raw spectra were analyzed using MetaboAnalyst 6.0 to create and annotate a peak list that was then used to perform untargeted lipidomics analysis [49]. Prior to performing statistical analysis, the data was filtered, normalized, transformed, and scaled (Fig. 5F). PCaP NP-treated macrophages were shown to possess a distinct lipidomic profile from either inactivated or classically activated macrophages (Fig. 5G, I, and Fig. S15). After observing this unique lipidomic signature, we sought to better understand which pathways were enriched in the PCaP NP-treated condition.

To accomplish this goal, pathway enrichment was performed using the MFN pathway library and several key pathways, including (i) carnitine shuttle ($P < 0.01$), (ii) vitamin E ($P < 0.01$), (iii) 3-oxo-10R octadecadienoate beta-oxidation ($P < 0.01$), (iv) glycolysis and gluconeogenesis ($P < 0.01$), (v) vitamin K metabolism ($P < 0.01$), (vi) linoleate metabolism ($P < 0.05$), and (vii) squalene and cholesterol biosynthesis ($P < 0.05$) were identified and found to be enriched in PCaP-treated classically activated macrophages (Fig. 5H). Each of these enriched pathways provide rationale for the metabolic shift away from a proinflammatory phenotype observed in the treated condition. The carnitine shuttle pathway is responsible for moving long-chain fatty acids, such as 3-oxo-10R-octadecadienoate, into the mitochondria, where they can be processed via β-oxidation to regenerate ATP at the end of the electron transport chain [50,51]. Moreover, linoleic acid has been shown to activate various receptors, including PPARγ, thereby promoting an anti-inflammatory phenotype and can also be used as an energy source via FAO [31]. While squalene is a precursor to cholesterol, this fatty acid has been implicated in literature to facilitate the resolution of wound healing by promoting anti-inflammatory signals (i.e., IL-10, IL-13, and IL-4) and encouraging tissue remodeling while suppressing pro-inflammatory signals (i.e., TNF-α and NF-κB) [52]. Lastly, the vitamin E metabolic pathway was shown to be enriched in our treated condition. The metabolism of this lipid-soluble antioxidant is known to suppress pro-inflammatory signals including NF-κB, scavenge

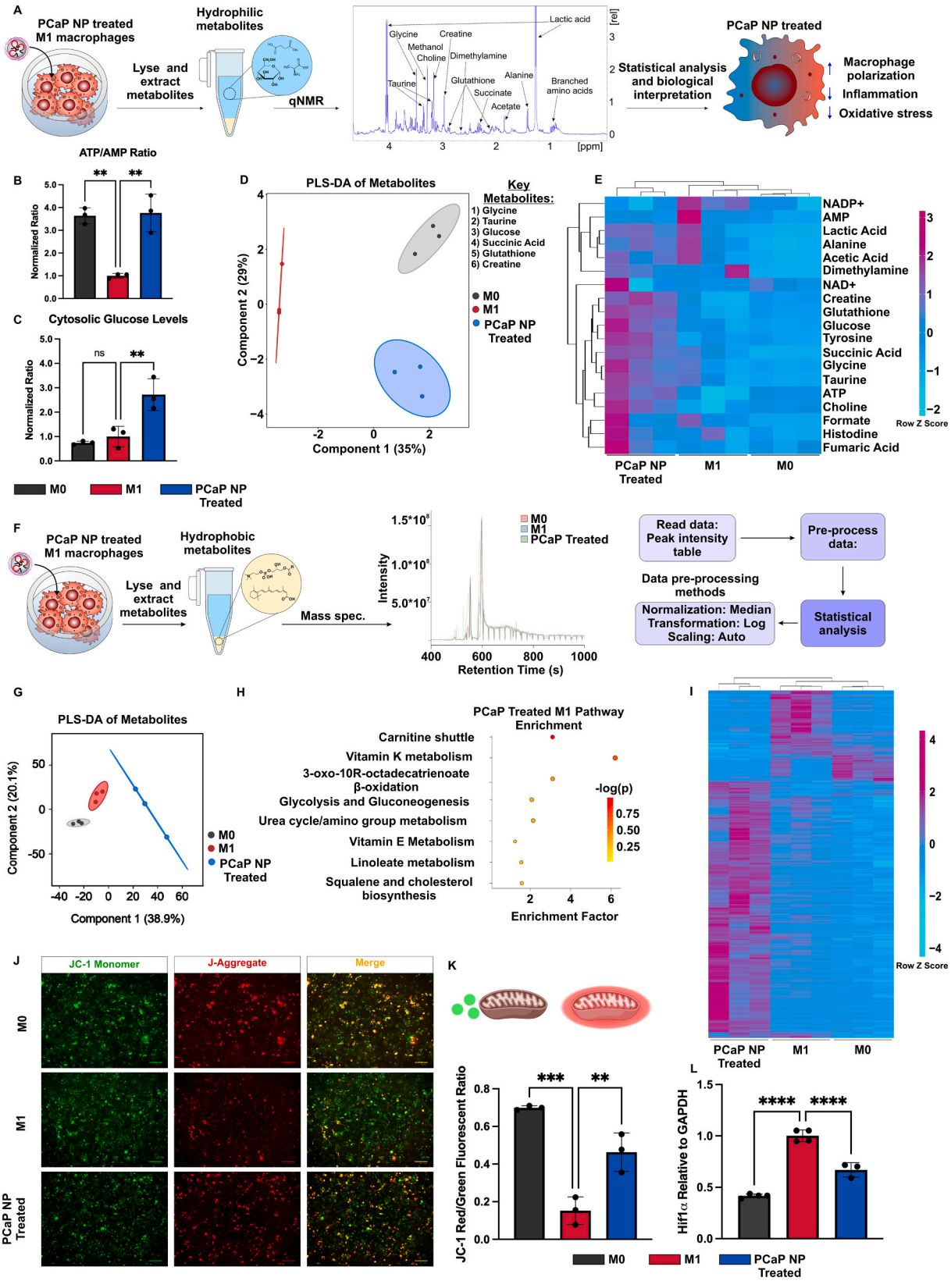

(caption on next page)

Fig. 5. PCaP NP-treated classically activated macrophages undergo shifts in metabolism and bioenergetics that are indicative of cellular health. A) Schematic depicting PCaP NP treatment to M1-like macrophages and extraction of water-soluble metabolites, representative qNMR spectra used to identify key metabolites, and schematic illustration of how these spectra are used to make biological interpretations about cellular behavior following treatment. B) Ratio of ATP: AMP demonstrating changes in bioenergetics following PCaP NP treatment ($n = 3$). C) Changes in glucose as quantified by qNMR. D) PLS-DA analysis and 95% confidence intervals demonstrating PCaP NP-treated classically activated macrophages are metabolically distinct from M1-like and inactivated macrophages. Important metabolites were identified via the PCA loading scores ($n = 3$). E) Heatmap depicting changes in individual metabolites quantified via NMR (n = 3). Scale = *Z*-score F) Schematic demonstration of the isolation of lipids from cellular extracts, representative mass spectrometry spectrum demonstrating differences in lipidomic profiles in M0, M1-like, and M1-like treated macrophages with PCaP NP. The data was subject to median normalization, log transformation, and auto scaled to create a normal distribution. G and H) PCA and pathway enrichment analysis of M1-like and M1-like treated macrophages (n = 3). I) Heatmap depicting M1-like treated macrophages have a lipidomic profile that is distinct from M0 and M1-like macrophages (n = 3). Scale = Z-score. J) Representative fluorescent microscopy images following JC-1 staining of M0, M1-like, and M1-like macrophages treated with PCaP NP. Scale bar = 100 μm. K) Quantification of JC-1 red: green ratio (n = 3). L) RT-qPCR of HIF-1α to further demonstrate mitochondrial health. Mean ± SEM, one-way ANOVA, turkey test, and *t*-test. $^{*}P < 0.05$; $^{**}P < 0.01$; $^{***}P < 0.001$.

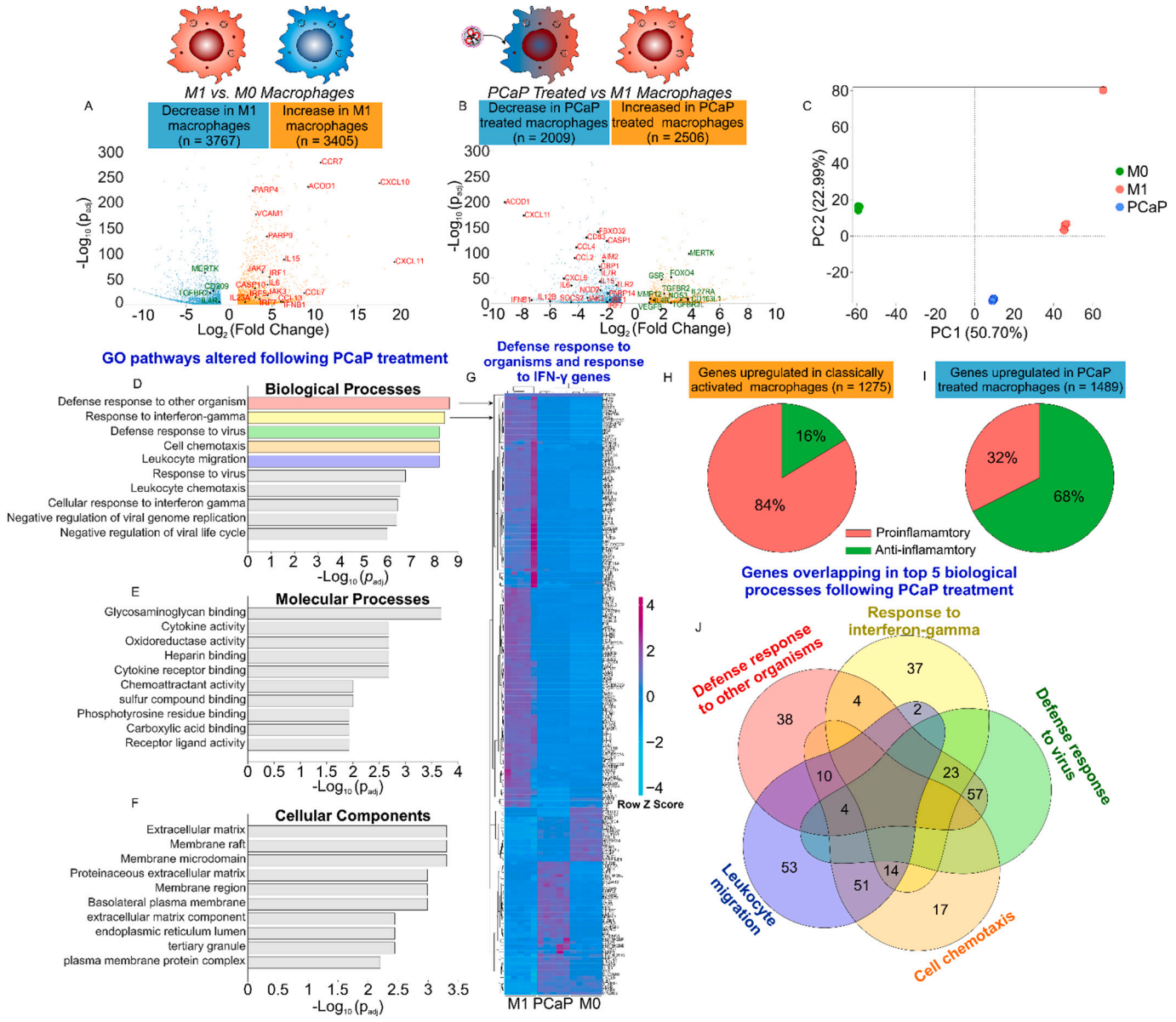

Fig. 6. Transcriptomic changes mediated by PCaP NP in classically activated treated macrophages. A and B) Volcano plots showing genes regulated in (A) classically activated versus inactivated macrophages and (B) classically activated versus PCaP NP treated classically activated macrophages ($n = 5$). Important cytokines, transcription factors, and biological markers are highlighted in red if they are pro-inflammatory or green if anti-inflammatory. C) PCA analysis demonstrating M0, M1-like, and M1-like treated macrophages possess distinct transcriptomic signatures (n = 5). D—F) Genes that were differentially expressed in M1-like treated macrophages compared to M1-like macrophages were entered into pathway analysis for (D) biological processes, (E) molecular processes, and (F) cellular processes (n = 5). The top 10 significant pathways for each category are depicted. (G) Heatmap demonstrating the genes involved in the top 2 biological processes "Defense response to other organisms" and "Response to interferon-gamma" (n = 5). Scale = *Z*-score of FPKM values. H and I) Pie charts demonstrating the percent of proinflammatory and anti-inflammatory genes regulated in classically activated and PCaP NP treated. J) Venn diagram showing the unique and overlapped genes in the top 5 biological processes.

radicals from reactive nitrogen species, and terminate lipid peroxidation [51,53]. Similarly, vitamin K, which was also enriched in our treated condition, is known to suppress inflammatory cytokine production and NF-κB activity [54].

2.4. Transcriptomic profiles of classically activated and PCaP NP treated macrophages

To gain insight into how the PCaP NP platform influences the transcriptomic profile of treated classically activated macrophages, we analyzed the inactivated, classically activated, and PCaP NP-treated classically activated macrophages using bulk RNA sequencing. Given the metabolomic changes that were observed in both the hydrophilic and hydrophobic metabolites, we expected to observe significant changes in the phenotype of treated cells. We noted that 24 h after activation, there was an increase in pro-inflammatory chemokines, chemokine receptors interleukins, vascular cell adhesion molecules, JAK-STAT activation, and transcription factors in the classically activated compared to inactivated macrophages (Fig. 6A). Similarly, anti-inflammatory signals such as *mertk*, *tgfβR2*, and *il4r* were down-regulated. However, treatment of classically activated macrophages with the PCaP NP platform significantly reduced pro-inflammatory mediators, such as interferons, cytokines, toll-like receptors, pro-inflammatory transcription factors, and caspase activity. Concurrently, the platform increased anti-inflammatory markers, including growth factors, interleukins, M2 macrophage polarization markers, tissue remodeling proteins, and anti-inflammatory transcription factors (Fig. 6B). In fact, principal component analysis reveals the treated activated macrophages adopt a phenotype that is distinct from either the inactivated and classically activated macrophages (Fig. 6C and Fig. S11).

Moreover, RNA-seq reveals that transcripts in the cholesterol biosynthesis pathway leading from acetyl-CoA to squalene are upregulated in the PCaP NP-treated condition while lanosterol synthase is down-regulated and should limit cholesterol synthesis (Fig. 6B).

Next, we determined what genes controlled the major biological processes most significantly affected following PCaP NP treatment, including defense response to other organisms and response to interferon-gamma, respectively (Fig. 6D, G, and Fig. S12). Following treatment with PCaP NP, the top five molecular functions that increased involved recognizing, responding to, and providing chemical signals in the environment. Specifically, these included (i) glycosaminoglycan binding, (ii) cytokine activity, (iii) oxidoreductase activity, (iv) heparin binding, and (v) cytokine receptor binding (Fig. 6E). Moreover, the top five cellular components affected by PCaP NP treatment in classically activated macrophages were related to extracellular signaling and include (i) extracellular matrix, (ii) membrane rafts, (iii) membrane microdomain, (iv) proteinaceous extracellular matrix, and (v) membrane region (Fig. 6F). Reactome pathway analysis also highlighted that PCaP NP-treated activated macrophages had alterations in the extracellular matrix organization, cytokine signaling, immune system, metabolism, and signal transduction (Supplemental Table 2). When comparing the genes that were differentially expressed between the PCaP NP-treated and classically activated conditions, there was a clear shift in the transcriptomic profile between these conditions. Of the genes involved in the inflammatory process, 84% of the differentially expressed genes (DEGs) in classically activated macrophages were pro-inflammatory, and only 16% were immunosuppressive (Fig. 6H). Conversely, in the PCaP NP-treated group, 68% of the DEGs displayed immunosuppressive characteristics, while only 32% were identified as immunoactive (Fig. 6I). Finally, the genes associated with the top five biological processes that were increased in classically activated macrophages following PCaP NP were organized in a Venn diagram and approximately 83.5% (259/310) of the genes were involved in 1 or 2 processes. The remaining 51 were involved in 3–4 processes, with only 4 genes (*cxcl10*, *cxcl9*, *il6*, and *lyst*) involved in 4 biological processes (Fig. 6J and Supplemental Table 3).

3. Conclusion and summary

In this study, we have successfully developed and characterized a synergistic nanoparticle platform composed of biodegradable and biocompatible materials to achieve efficient intracellular delivery of DNAzymes into macrophages. In classically activated macrophages, IRF5 supports a pro-inflammatory, glycolysis-dependent metabolic state, that elevates cytokine production and sustains an inflammatory milieu. By reducing IRF5 expression, we effectively redirect the cellular energy balance toward oxidative phosphorylation and improve mitochondrial health. This metabolic reprogramming indicates a shift away from a pro-inflammatory phenotype. Such a shift is significant at the cellular level and has broader implications in treating conditions driven by chronic inflammation. Traditional therapeutic approaches often involve systemic immunosuppression or broad-spectrum anti-inflammatory drugs that carry the risk of severe side effects and reduced specificity [55]. Our nanoparticle-based platform circumvents these limitations by providing an efficient and tunable method of modulating macrophage polarization. This precision approach may enhance tissue repair, reduce pathological inflammation, and improve the overall outcomes in various chronic inflammatory conditions.

By employing CaP nanoparticles coated with an ionizable polymer, our platform ensures the stable encapsulation of 10–23 DNAzymes, their transport into the macrophage cytoplasm, and their subsequent activation under physiologically relevant conditions. Unlike traditional RNA interference (RNAi)-based systems, which often depend on multiple endogenous factors and are vulnerable to rapid enzymatic degradation, DNAzymes require only a divalent metal ion cofactor for catalytic activity and are inherently less immunogenic. This reduced immunogenicity is critical in cells like macrophages which possess a wide array of pattern recognition receptors and cytosolic sensors, such as cGAS-STING that can trigger innate immune responses upon detecting foreign nucleic acids. Furthermore, the CaP nanoparticle core not only protects the DNAzyme cargo from degradation by extracellular and intracellular nucleases but also provides a continuous source of divalent calcium ions that enhance DNAzyme activity while PBAE facilitates cellular uptake and endosomal escape of the nanoparticles.

From a translational perspective, our technology platform can be readily adapted to deliver different DNAzymes or other nucleic acid-based therapeutics for distinct molecular targets. Such adaptability broadens the spectrum of possible clinical applications and allows for rapidly customizing therapies for specific disease contexts. In our case, the PCaP NPs should translate fluidly from in vitro to in vivo investigations. Our therapeutic platform is entirely biodegradable to ensure full renal clearance, which is typically problematic with many NP-based platforms. Secondly, the degraded components of our system have been shown to be non-toxic and ultimately biocompatible from a biosafety point of view. Lastly, our platform has been shown to resist degradation over a 4–6 day period of time, ensuring good bioavailability for the therapeutic to reach its intended target. Once reached, the acidic microenvironment of the endosome will facilitate the NP's dissolution and release the nucleic acid payload to provide the intended therapeutic function. However, our platform is currently optimized for in vitro studies and still requires further design for optimal in vivo testing. For example, in the complex in vivo biological environment, it would be crucial to incorporate a targeting ligand on the PCaP NP for macrophage-honing to ensure high efficacy of the therapeutic. Due to the modular design of our system, modifying the PBAE polymer coating of the NP with such a ligand would be entirely feasible and likely not affect the biodegradable characteristics of the system. In this way, we hypothesize that the design of our PCaP NP system allows for modular tuning which would facilitate a transition to a more clinically-relevant in vivo investigation. Although we have not explored in vivo testing for our platform in the scope of this manuscript, we intend to venture into such translational testing in future works.

In summary, our work presents a robust and innovative strategy for

reprogramming macrophages away from a pro-inflammatory phenotype. By delivering and activating a 10–23 DNAzyme targeting IRF5 with our carefully designed platform, we significantly reduced pro-inflammatory cytokine production through modulating key inflammatory pathways. This approach may offer novel therapeutic avenues for managing chronic inflammatory diseases, such as autoimmune disorders and metabolic syndrome, and has the potential to improve wound healing outcomes significantly. Beyond macrophage reprogramming, the principles established here, including precise targeting, minimal immunogenicity, controlled activation, and phenotypic modulation, can be extended to other immune cells and inflammatory mediators. Ultimately, this nanoparticle-based platform has the potential to revolutionize the development of next-generation immunomodulatory therapies.

CRediT authorship contribution statement

Brandon Conklin: Writing – original draft, Visualization, Formal analysis, Data curation, Conceptualization. **Sarah Nevins:** Writing – review & editing, Formal analysis, Data curation. **Callan D. McLoughlin:** Writing – review & editing, Formal analysis, Data curation. **Skylar T. Chuang:** Conceptualization. **Joshua B. Stein:** Formal analysis, Data curation. **Yannan Hou:** Formal analysis, Data curation. **Munaifa Arif:** Formal analysis, Data curation. **Mehdi Kamali:** Formal analysis, Data curation. **Ki-Bum Lee:** Supervision, Project administration, Funding acquisition.

Declaration of competing interest

The authors declare that they have no known competing financial interests or personal relationships that could have appeared to influence the work reported in this paper.

Acknowledgements

Ki-Bum Lee acknowledges the partial financial support from the NSF (CBET-1803517), the New Jersey Commission on Spinal Cord Research (CSCR17IRG010; CSCR16ERG019; CSCR22ERG023), NIH R21 (R21AR071101), and NIH R01 (1R01DC016612, 1R01NS130836-01A1, 3R01DC016612-01S1, and 5R01DC016612-02S1), NIH RM1 (RM1 NS133003-01), NIH R21 (R21 NS132556-01), Alzheimer's Association (AARG-NTF-21-847862), CDMRP (OCRP, OC220235P1). Brandon Conklin acknowledges fellowship support as part of the NIH T32 Training in Translating Neuroscience to Therapies program (5T32NS115700-02). Sarah Nevins acknowledges fellowship support as part of the NIH T32 Biotechnology Training Program (GM135141). The authors acknowledge the use of Biorender for the creation of figures.

Appendix A. Supplementary data

Supplementary data to this article can be found online at https://doi.org/10.1016/j.cej.2026.173835.

Data availability

Data will be made available on request.

References

[1] L. Chang-Hoon, C. Eun Young, Macrophages and Inflammation, J Rheum Dis 25 (1) (2018) 11–18, https://doi.org/10.4078/jrd.2018.25.1.11.
[2] C. He, A.B. Carter, The metabolic prospective and redox regulation of macrophage polarization, J Clin Cell Immunol 6 (6) (2015), https://doi.org/10.4172/2155-9899.1000371.
[3] G.C. Gurtner, S. Werner, Y. Barrandon, M.T. Longaker, Wound repair and regeneration, Nature 453 (7193) (2008) 314–321, https://doi.org/10.1038/nature07039.
[4] H. Zhang, Y. Yu, C. Qian, Oligonucleotide-based modulation of macrophage polarization: emerging strategies in immunotherapy, Immun Inflamm Dis 13 (5) (2025) e70200, https://doi.org/10.1002/iid3.70200.
[5] R.G. Frykberg, J. Banks, Challenges in the treatment of chronic wounds, Adv. Wound Care 4 (9) (2015) 560–582, https://doi.org/10.1089/wound.2015.0635.
[6] K.A. Fitzgerald, J.C. Kagan, Toll-like receptors and the control of immunity, Cell 180 (6) (2020) 1044–1066, https://doi.org/10.1016/j.cell.2020.02.041.
[7] R. Bayraktar, M.T.S. Bertilaccio, G.A. Calin, The interaction between two worlds: MicroRNAs and toll-like receptors, Front. Immunol. 10 (2019), https://doi.org/10.3389/fimmu.2019.01053.
[8] M. Motwani, S. Pesiridis, K.A. Fitzgerald, DNA sensing by the cGAS–STING pathway in health and disease, Nat. Rev. Genet. 20 (11) (2019) 657–674, https://doi.org/10.1038/s41576-019-0151-1.
[9] M. Winkle, S.M. El-Daly, M. Fabbri, G.A. Calin, Noncoding RNA therapeutics — challenges and potential solutions, Nat. Rev. Drug Discov. 20 (8) (2021) 629–651, https://doi.org/10.1038/s41573-021-00219-z.
[10] G.F. Joyce, Methods in Enzymology, Academic Press, in: A.W. Nicholson (Ed.), [32] - RNA Cleavage by the 10–23 DNA Enzyme, 2001, pp. 503–517, https://doi.org/10.1016/S0076-6879(01)41173-6.
[11] A. de Fougerolles, H.-P. Vornlocher, J. Maraganore, J. Lieberman, Interfering with disease: a progress report on siRNA-based therapeutics, Nat. Rev. Drug Discov. 6 (6) (2007) 443–453, https://doi.org/10.1038/nrd2310.
[12] S.W. Santoro, G.F. Joyce, Mechanism and utility of an RNA-cleaving DNA enzyme, Biochemistry 37 (38) (1998) 13330–13342, https://doi.org/10.1021/bi9812221.
[13] U. Ohto, H. Ishida, T. Shibata, R. Sato, K. Miyake, T. Shimizu, Toll-like receptor 9 contains two DNA binding sites that function cooperatively to promote receptor dimerization and activation, Immunity 48 (4) (2018) 649–658.e4, https://doi.org/10.1016/j.immuni.2018.03.013.
[14] D.P. Potaczek, S.D. Unger, N. Zhang, S. Taka, S. Michel, N. Akdağ, F. Lan, M. Helfer, C. Hudemann, M. Eickmann, C. Skevaki, S. Megremis, A. Sadewasser, B. Alashkar Alhamwe, F. Alhamdan, M. Akdis, M.R. Edwards, S.L. Johnston, C. A. Akdis, S. Becker, C. Bachert, N.G. Papadopoulos, H. Garn, H. Renz, Development and characterization of DNAzyme candidates demonstrating significant efficiency against human rhinoviruses, J. Allergy Clin. Immunol. 143 (4) (2019) 1403–1415, https://doi.org/10.1016/j.jaci.2018.07.026.
[15] T. Dicke, I. Pali-Schöll, A. Kaufmann, S. Bauer, H. Renz, H. Garn, Absence of unspecific innate immune cell activation by GATA-3-specific DNAzymes, Nucleic Acid Ther. 22 (2) (2012) 117–126, https://doi.org/10.1089/nat.2011.0294.
[16] Y. Wang, K. Nguyen, R.C. Spitale, J.C. Chaput, A biologically stable DNAzyme that efficiently silences gene expression in cells, Nat. Chem. 13 (4) (2021) 319–326, https://doi.org/10.1038/s41557-021-00645-x.
[17] J. Yan, M. Ran, X. Shen, H. Zhang, Therapeutic DNAzymes: from structure design to clinical applications, Adv. Mater. 35 (30) (2023) 2300374, https://doi.org/10.1002/adma.202300374.
[18] H.L. Eames, D.G. Saliba, T. Krausgruber, A. Lanfrancotti, G. Ryzhakov, I. A. Udalova, KAP1/TRIM28: an inhibitor of IRF5 function in inflammatory macrophages, Immunobiology 217 (12) (2012) 1315–1324, https://doi.org/10.1016/j.imbio.2012.07.026.
[19] T. Krausgruber, K. Blazek, T. Smallie, S. Alzabin, H. Lockstone, N. Sahgal, T. Hussell, M. Feldmann, I.A. Udalova, IRF5 promotes inflammatory macrophage polarization and TH1-TH17 responses, Nat. Immunol. 12 (3) (2011) 231–238, https://doi.org/10.1038/ni.1990.
[20] T. Krausgruber, K. Blazek, T. Smallie, S. Alzabin, H. Lockstone, N. Sahgal, T. Hussell, M. Feldmann, I.A. Udalova, IRF5 promotes inflammatory macrophage polarization and TH1-TH17 responses, Nat. Immunol. 12 (3) (2011) 231–238, https://doi.org/10.1038/ni.1990.
[21] M. Hedl, J. Yan, C. Abraham, IRF5 and IRF5 disease-risk variants increase glycolysis and human M1 macrophage polarization by regulating proximal signaling and Akt2 activation, Cell Rep. 16 (9) (2016) 2442–2455, https://doi.org/10.1016/j.celrep.2016.07.060.
[22] Y. Lee, M. Jeong, J. Park, H. Jung, H. Lee, Immunogenicity of lipid nanoparticles and its impact on the efficacy of mRNA vaccines and therapeutics, Exp. Mol. Med. 55 (10) (2023) 2085–2096, https://doi.org/10.1038/s12276-023-01086-x.
[23] K. Sato, M. Akiyama, Y. Sakakibara, RNA secondary structure prediction using deep learning with thermodynamic integration, Nat. Commun. 12 (1) (2021) 941, https://doi.org/10.1038/s41467-021-21194-4.
[24] A.C. Pine, G.N. Brooke, A. Marco, A computational approach to identify efficient RNA cleaving 10-23 DNAzymes, NAR Genom Bioinform 5 (1) (2023) lqac098, https://doi.org/10.1093/nargab/lqac098.
[25] K. Nguyen, T.N. Malik, J.C. Chaput, Chemical evolution of an autonomous DNAzyme with allele-specific gene silencing activity, Nat. Commun. 14 (1) (2023) 2413, https://doi.org/10.1038/s41467-023-38100-9.
[26] Z. Zaborowska, J.P. Fürste, V.A. Erdmann, J. Kurreck, Sequence requirements in the catalytic core of the "10-23" DNA enzyme, J. Biol. Chem. 277 (43) (2002) 40617–40622, https://doi.org/10.1074/jbc.M207094200.
[27] T.T. Morgan, H.S. Muddana, E.I. Altinoglu, S.M. Rouse, A. Tabaković, T. Tabouillot, T.J. Russin, S.S. Shanmugavelandy, P.J. Butler, P.C. Eklund, J. K. Yun, M. Kester, J.H. Adair, Encapsulation of organic molecules in calcium phosphate nanocomposite particles for intracellular imaging and drug delivery, Nano Lett. 8 (12) (2008) 4108–4115, https://doi.org/10.1021/nl8019888.
[28] Y.-W. Chao, Y.-L. Lee, C.-S. Tseng, L.U.-H. Wang, K.-C. Hsia, H. Chen, J.-M. Fustin, S. Azeem, T.-T. Chang, C.-Y. Chen, F.-C. Kung, Y.-P. Hsueh, Y.-S. Huang, H.-W. Chao, Improved CaP nanoparticles for nucleic acid and protein delivery to neural primary cultures and stem cells, ACS Nano 18 (6) (2024) 4822–4839, https://doi.org/10.1021/acsnano.3c09608.

[29] C.R. Mendes, G. Dilarri, C.F. Forsan, V.d.M.R. Sapata, P.R.M. Lopes, P.B. de Moraes, R.N. Montagnolli, H. Ferreira, E.D. Bidoia, Antibacterial action and target mechanisms of zinc oxide nanoparticles against bacterial pathogens, Sci. Rep. 12 (1) (2022) 2658, https://doi.org/10.1038/s41598-022-06657-y.
[30] S.A. Read, S. Obeid, C. Ahlenstiel, G. Ahlenstiel, The role of zinc in antiviral immunity, Adv. Nutr. 10 (4) (2019) 696–710, https://doi.org/10.1093/advances/nmz013.
[31] S. Zhang, K. Lv, Z. Liu, R. Zhao, F. Li, Fatty acid metabolism of immune cells: a new target of tumour immunotherapy, Cell Death Discov. 10 (1) (2024) 39, https://doi.org/10.1038/s41420-024-01807-9.
[32] L. Peng, H. Zhang, Y. Hao, F. Xu, J. Yang, R. Zhang, G. Lu, Z. Zheng, M. Cui, C.-F. Qi, C. Chen, J. Wang, Y. Hu, D. Wang, S. Pierce, L. Li, H. Xiong, Reprogramming macrophage orientation by microRNA 146b targeting transcription factor IRF5, eBioMedicine 14 (2016) 83–96, https://doi.org/10.1016/j.ebiom.2016.10.041.
[33] C. Guo, W. Kong, K. Kamimoto, G.C. Rivera-Gonzalez, X. Yang, Y. Kirita, S. A. Morris, CellTag Indexing: genetic barcode-based sample multiplexing for single-cell genomics, Genome Biol. 20 (1) (2019) 90, https://doi.org/10.1186/s13059-019-1699-y.
[34] W. Kong, B.A. Biddy, K. Kamimoto, J.M. Amrute, E.G. Butka, S.A. Morris, CellTagging: combinatorial indexing to simultaneously map lineage and identity at single-cell resolution, Nat. Protoc. 15 (3) (2020) 750–772, https://doi.org/10.1038/s41596-019-0247-2.
[35] J.I.I.I. Forster, D. Nandi, A. Kulkarni, mRNA-carrying lipid nanoparticles that induce lysosomal rupture activate NLRP3 inflammasome and reduce mRNA transfection efficiency, Biomater Sci-Uk 10 (19) (2022) 5566–5582, https://doi.org/10.1039/d2bm00883a.
[36] P.D. Pozniak, M.K. White, K. Khalili, TNF-α/NF-κB signaling in the CNS: possible connection to EPHB2, J. NeuroImmune Pharmacol. 9 (2) (2014) 133–141, https://doi.org/10.1007/s11481-013-9517-x.
[37] Z. Zhong, A. Umemura, E. Sanchez-Lopez, S. Liang, S. Shalapour, J. Wong, F. He, D. Boassa, G. Perkins, S.R. Ali, M.D. McGeough, M.H. Ellisman, E. Seki, A. B. Gustafsson, H.M. Hoffman, M.T. Diaz-Meco, J. Moscat, M. Karin, NF-κB restricts Inflammasome activation via elimination of damaged mitochondria, Cell 164 (5) (2016) 896–910, https://doi.org/10.1016/j.cell.2015.12.057.
[38] M. Obaid, S.M.N. Udden, P. Alluri, S.S. Mandal, LncRNA HOTAIR regulates glucose transporter Glut1 expression and glucose uptake in macrophages during inflammation, Sci. Rep. 11 (1) (2021) 232, https://doi.org/10.1038/s41598-020-80291-4.
[39] B. Kelly, L.A.J. O'Neill, Metabolic reprogramming in macrophages and dendritic cells in innate immunity, Cell Res. 25 (7) (2015) 771–784, https://doi.org/10.1038/cr.2015.68.
[40] E.L. Mills, L.A. O'Neill, Reprogramming mitochondrial metabolism in macrophages as an anti-inflammatory signal, Eur. J. Immunol. 46 (1) (2016) 13–21, https://doi.org/10.1002/eji.201445427.
[41] E. Hickman, T. Smyth, C. Cobos-Uribe, R. Immormino, M.E. Rebuli, T. Moran, N. E. Alexis, I. Jaspers, Expanded characterization of in vitro polarized M0, M1, and M2 human monocyte-derived macrophages: bioenergetic and secreted mediator profiles, PLoS One 18 (3) (2023) e0279037, https://doi.org/10.1371/journal.pone.0279037.
[42] F. Wang, S. Zhang, I. Vuckovic, R. Jeon, A. Lerman, C.D. Folmes, P.P. Dzeja, J. Herrmann, Glycolytic stimulation is not a requirement for M2 macrophage differentiation, Cell Metab. 28 (3) (2018) 463–475.e4, https://doi.org/10.1016/j.cmet.2018.08.012.
[43] Z. Gan, M. Zhang, D. Xie, X. Wu, C. Hong, J. Fu, L. Fan, S. Wang, S. Han, Glycinergic signaling in macrophages and its application in macrophage-associated diseases, Front. Immunol. 12 (2021), https://doi.org/10.3389/fimmu.2021.762564.
[44] L. Meng, C. Lu, B. Wu, C. Lan, L. Mo, C. Chen, X. Wang, N. Zhang, L. Lan, Q. Wang, X. Zeng, X. Li, S. Tang, Taurine antagonizes macrophages M1 polarization by Mitophagy-glycolysis switch blockage via dragging SAM-PP2Ac Transmethylation, Front. Immunol. 12 (2021) 648913, https://doi.org/10.3389/fimmu.2021.648913.
[45] T. Shen, R. Lin, C. Hu, D. Yu, C. Ren, T. Li, M. Zhu, Z. Wan, T. Su, Y. Wu, W. Cai, J. Yu, Succinate-induced macrophage polarization and RBP4 secretion promote vascular sprouting in ocular neovascularization, J. Neuroinflammation 20 (1) (2023) 308, https://doi.org/10.1186/s12974-023-02998-1.
[46] Y. Li, X. Jin, X. Yang, L. Zhang, Z. Qi, Creatine promotes the repair of peripheral nerve injury by affecting macrophage polarization, Biochem. Biophys. Res. Commun. 604 (2022) 116–122, https://doi.org/10.1016/j.bbrc.2022.03.047.
[47] D.H. Kwon, H. Lee, C. Park, S.H. Hong, S.H. Hong, G.Y. Kim, H.J. Cha, S. Kim, H. S. Kim, H.J. Hwang, Y.H. Choi, Glutathione induced immune-stimulatory activity by promoting M1-like macrophages polarization via potential ROS scavenging capacity, Antioxidants-Basel 8 (9) (2019) doi:ARTN41310.3390/antiox8090413.
[48] J.D. Ly, D.R. Grubb, A. Lawen, The mitochondrial membrane potential (Δψm) in apoptosis; an update, Apoptosis 8 (2) (2003) 115–128, doi:10.1023/A:1022945107762.
[49] Z. Pang, Y. Lu, G. Zhou, F. Hui, L. Xu, C. Viau, Aliya F. Spigelman, Patrick E. MacDonald, David S. Wishart, S. Li, J. Xia, MetaboAnalyst 6.0: towards a unified platform for metabolomics data processing, analysis and interpretation, Nucleic Acids Res. 52 (W1) (2024) W398–W406, https://doi.org/10.1093/nar/gkae253.
[50] N. Longo, M. Frigeni, M. Pasquali, Carnitine transport and fatty acid oxidation, Biochim. Biophys. Acta 1863 (10) (2016) 2422–2435, https://doi.org/10.1016/j.bbamcr.2016.01.023.
[51] N.J.W. Rattray, D.K. Trivedi, Y. Xu, T. Chandola, C.H. Johnson, A.D. Marshall, K. Mekli, Z. Rattray, G. Tampubolon, B. Vanhoutte, I.R. White, F.C.W. Wu, N. Pendleton, J. Nazroo, R. Goodacre, Metabolic dysregulation in vitamin E and carnitine shuttle energy mechanisms associate with human frailty, Nat. Commun. 10 (1) (2019) 5027, https://doi.org/10.1038/s41467-019-12716-2.
[52] C. Sánchez-Quesada, A. López-Biedma, E. Toledo, J.J. Gaforio, Squalene stimulates a key innate immune cell to Foster wound healing and tissue repair, Evid. Based Complement. Alternat. Med. 2018 (2018) 9473094, https://doi.org/10.1155/2018/9473094.
[53] E.D. Lewis, S.N. Meydani, D. Wu, Regulatory role of vitamin E in the immune system and inflammation, IUBMB Life 71 (4) (2019) 487–494, https://doi.org/10.1002/iub.1976.
[54] N. Karamzad, V. Maleki, K. Carson-Chahhoud, S. Azizi, A. Sahebkar, B.P. Gargari, A systematic review on the mechanisms of vitamin K effects on the complications of diabetes and pre-diabetes, Biofactors 46 (1) (2020) 21–37, https://doi.org/10.1002/biof.1569.
[55] S. Bindu, S. Mazumder, U. Bandyopadhyay, Non-steroidal anti-inflammatory drugs (NSAIDs) and organ damage: a current perspective, Biochem. Pharmacol. 180 (2020) doi:ARTN11414710.1016/j.bcp.2020.114147.